Title

Hypoxia-related carbonic anhydrase 9 induces serpinB9 expression in cancer cells and apoptosis in T cells via acidosis

Author(s)

Mamoru Harada, Hitoshi Kotani, Yuichi Iida, Ryosuke Tanino, Takafumi Minami, Yoshihiro Komohara, Kazuhiro Yoshikawa, and Hirotsugu Uemura

Hypoxia-related carbonic anhydrase 9 induces serpinB9 expression in cancer cells and apoptosis in T cells via acidosis

SCHOLARONE™
Manuscripts

Hypoxia-related carbonic anhydrase 9 induces serpinB9 expression in cancer cells and apoptosis in T cells via acidosis

Mamoru Harada,[1]* Hitoshi Kotani,[1] Yuichi Iida,[1] Ryosuke Tanino,[2] Takafumi Minami,[3] Yoshihiro Komohara,[4] Kazuhiro Yoshikawa,[5] and Hirotsugu Uemura[3]

[1] Department of Immunology, Shimane University Faculty of Medicine, Shimane, Japan.

[2] Division of Medical Oncology & Respiratory Medicine, Department of Internal Medicine, Shimane University Faculty of Medicine, Shimane, Japan.

[3] Department of Urology, Kindai University Faculty of Medicine, Osaka, Japan.

[4] Department of Cell Pathology, Graduate School of Medical Science, Kumamoto University, Kumamoto, Japan.

[5] Research Creation Support Center, Aichi Medical University, Aichi, Japan.

Correspondence: Mamoru Harada, Department of Immunology, Shimane University Faculty of Medicine, Izumo, Shimane 693-8501, Japan

E-mail: haramamo@med.shimane-u.ac.jp

Keywords: hypoxia, carbonic anhydrase 9, serpin B9, acidosis

Word count (excluding references): 5742 words

Number of tables/figures: 0 table, 6 figures

Quantity of supplementary data: 5

1

1
2
3
4
5
6
7
8
9
10
11
12
13
14
15
16
17
18
19
20
21
22
23
24
25
26
27
28
29
30
31
32
33
34
35
36
37
38
39
40
41
42
43
44
45
46
47
48
49
50
51
52
53
54
55
56
57
58
59
60

27   **ABSTRACT**

28

29   Hypoxia is a common feature of solid tumors. However, the impact of hypoxia on

30   immune cells within tumor environments remains underexplored. Carbonic anhydrase 9

31   (CA9) is a hypoxia-responsive tumor-associated enzyme. We previously noted that

32   regardless of human CA9 (hCA9) expression, hCA9-expressing mouse renal cell

33   carcinoma RENCA (RENCA/hCA9) presented as a 'cold' tumor in syngeneic aged mice.

34   This study delves into the mechanisms behind this observation. Gene microarray analyses

35   showed that RENCA/hCA9 cells exhibited elevated mouse serpinB9, an inhibitor of

36   granzyme B, relative to RENCA cells. Corroborating this, RENCA/hCA9 cells displayed

37   heightened resistance to antigen-specific cytotoxic T cells compared to RENCA cells.

38   Notably, siRNA-mediated serpinB9 knockdown reclaimed this sensitivity. *In vivo* tests

39   showed that serpinB9 inhibitor administration slowed RENCA tumor growth, but this

40   effect was reduced in RENCA/hCA9 tumors, even with adjunctive immune checkpoint

41   blockade therapy. Further, inducing hypoxia or introducing the mouse CA9 gene

42   upregulated serpinB9 expression and siRNA-mediated knockdown of mouse *CA9* gene

43   inhibited the hypoxia-induced induction of serpinB9 in the original RENCA cells.

44   Supernatants from RENCA/hCA9 cultures had lower pH than those from RENCA,

45   suggesting acidosis. This acidity enhanced serpinB9 expression and T cell apoptosis.

46   Moreover, co-culturing with RENCA/hCA9 cells more actively prompted T cell

47   apoptosis than with RENCA cells. Collectively, these findings suggest hypoxia-

48   associated CA9 not only boosts serpinB9 in cancer cells but also synergistically

49   intensifies T cell apoptosis via acidosis, characterizing RENCA/hCA9 tumors as 'cold.'

50

51

2

1
2
3
4
5
6
7
8
9
10
11
12
13
14
15
16
17
18
19
20
21
22
23
24
25
26
27
28
29
30
31
32
33
34
35
36
37
38
39
40
41
42
43
44
45
46
47
48
49
50
51
52
53
54
55
56
57
58
59
60

1. INTRODUCTION

52

53

54 Immune checkpoint blockade (ICB) therapy has garnered widespread approval as an

55 effective treatment for various types of cancers.[1,2] Yet, its therapeutic efficacy depends

56 on the presence of immune cells, particularly CD8^{+} T cells, at tumor sites. Tumors that

57 display little or no immune cell infiltration, termed 'cold' tumors, pose a significant

58 challenge for achieving desired outcomes in cancer patients post-ICB therapy.[3,4] Thus, it

59 becomes imperative to determine why certain tumors hinder immune cell infiltration. To

60 address this, understanding the intricacies of the tumor microenvironment is essential.

61 Beyond immunosuppressive cells like regulatory T (Treg) cells and myeloid-derived

62 suppressor cells (MDSCs), the most pronounced features of the tumor microenvironment

63 include hypoxia and acidosis.[5,6] Such conditions can instigate the epithelial–

64 mesenchymal transition (EMT) in cancer cells[7] and increase their resistance against

65 cytotoxic immune cells.[8] Likely, hypoxia and acidosis contribute to the characteristics of

66 'cold' tumors.

67   Among various hypoxia-associated molecules,[9] carbonic anhydrase (CA) 9 stands

68 out.[10] Given its expression across diverse cancer types,[11] CA9 may serve as a tumor-

69 associated antigen for renal cell carcinoma (RCC). Indeed, CA9-derived peptides

70 recognized by cytotoxic T lymphocytes (CTLs) have been employed in cancer vaccine

71 strategies.[12] Moreover, despite a 30% amino acid sequence disparity between human CA9

72 (hCA9) and mouse CA9, we recently found that immune cell infiltration was markedly

73 reduced in hCA9-expressing mouse RCC RENCA (RENCA/hCA9) tissues compared to

74 the parent RENCA tissues in syngeneic aged mice.[13] Additionally, CA9, a hypoxia-

75 triggered tumor-associated cell surface enzyme, can acidify the tumor environment.[14,15]

76 Considering the roles of hypoxia and acidosis in limiting immune cell infiltration into

3

77 tumors, understanding why RENCA/hCA9 tissues manifest as 'cold' becomes essential.

78 In this study, we sought to uncover the mechanisms behind the suppressed immune

79 cell infiltration in RENCA/hCA9 tissues. Gene microarray analysis highlighted a higher

80 expression of serpinB9, a granzyme B inhibitor,[16] in RENCA/hCA9 cells compared to

81 RENCA cells. Our findings indicate that, through acidification, hypoxia-associated CA9

82 boosts serpinB9 expression, making cancer cells more resilient to antigen-specific CTLs,

83 and encourages T cell apoptosis via acidification.

84

2. MATERIALS AND METHODS

86

2.1 Mice, cell lines, and reagents

88 Young (6–7 weeks old) and aged (60 weeks old) BALB/c female mice were sourced from

89 CLEA (Tokyo, Japan). Mice were kept under specific pathogen-free conditions. All

90 experiments adhered to the ethical guidelines for animal research at Shimane University

91 Faculty of Medicine (IZ3-128, IZ5-52). RENCA is an RCC derived from BALB/c mice;

92 RENCA/hCA9 is a RENCA-derived cell line expressing hCA9.[17] RENCA/hCA9 was

93 established via transfection of the cloned human *CA9* gene (under the control of the

94 cytomegalovirus promoter/enhancer) in the pBCMGSneo vector.[18] Three other RENCA

95 cell lines stably expressing the human *CA9* gene were established via transfection of a

96 pCMV3-hCA9 vector in which hCA9 expression was controlled by the cytomegalovirus

97 promoter/enhancer (Sino Biological Inc.). All cell cultures thrived in RPMI 1640 medium

98 (Sigma-Aldrich, St. Louis, MO, USA) enhanced with 10% fetal bovine serum and 20

99 µg/mL gentamycin (Sigma-Aldrich). For some tests, RPMI-1640 medium without

100 sodium bicarbonate (SB) NaHCO$_3$ (Sigma-Aldrich) was chosen to negate any buffer

101 effects in the CO$_2$ incubator. The anti-PD-1 monoclonal antibody (mAb) (clone RMP 1-

4

102 14) and anti-CTLA-4 mAb (UC10-4F10-7) were sourced from Bio X Cell Inc. (Lebanon,

103 NH, USA). Deferoxamine (DFO) mesylate, an iron chelator, was procured from Wako

104 Chemical.

105 **2.2 Flow cytometry**

106 To evaluate tumor-infiltrating immune cells, tumors were first fragmented using glass

107 slides, then filtered through gauze mesh and nylon mesh prior to flow cytometry. The

108 following mAbs were used: APC-conjugated anti-CD45 mAb (BioLegend), FITC-

109 conjugated anti-CD8 mAb (BioLegend), PE-conjugated anti-CD4 mAb (BioLegend),

110 FITC-conjugated anti-F4/80 (BioLegend), and PE-conjugated anti-CD11b mAb

111 (BioLegend). Analysis was conducted on a FACSCalibur (Becton–Dickinson, Franklin

112 Lakes, NJ, USA). T cells were prepared from BALB/c spleen cells. After RBC lysis using

113 Lysis Buffer (ChemCruz), cells were stained with an anti-CD19 mAb (rat IgG,

114 BioLegend), washed, and incubated on ice for 30 min with DynaBeads Sheep Anti-Rat

115 IgG (Invitrogen). Cells that were not captured by a magnet (Invitrogen) were collected;

116 these collected cells displayed T-cell enrichment. These T cells were co-cultured with

117 cancer cells for intervals of 2 or 4 days. After culturing, the cells were tagged with PE-

118 conjugated anti-CD4 mAb (BioLegend) and APC-conjugated anti-CD8 mAb

119 (BioLegend), subsequently paired with FITC-conjugated annexin V, and analyzed using

120 CytoFLEX (Beckman Coulter). In specific experiments, T cells experienced varied pH

121 conditions during culturing. For analysis of apoptotic cancer cells under diverse pH

122 conditions, cells were labeled with FITC-conjugated annexin V and propidium iodide (PI)

123 (BioVision), then subjected to CytoFLEX flow cytometry.

124 **2.3 Transcriptome analysis**

125 Total RNA was extracted from RENCA and RENCA/hCA9 cells using the NucleoSpin

126 miRNA kit (MACHEREY-NAGEL). Gene expression profiling was conducted with the

5

127 Clariom D assay, Mouse (Thermo Fisher Scientific, Waltham, MA, USA). Chips were

128 scanned and image analyses were executed using the GeneChip Scanner 3000 7G

129 (Thermo Fisher Scientific) paired with the Expression Console Software (Thermo Fisher

130 Scientific). The gene-level signal space transformation-robust multiarray analysis method

131 was deployed for normalization, facilitating gene expression comparison between groups.

132 Gene Ontology enrichment analysis was carried out using Metascape version 3.5.[19]

133 2.4 Gene expression variation analysis on 43 human renal cell lines

134 A publicly available RNA-seq gene expression dataset was sourced from the Cancer Cell

135 Line Encyclopedia (CCLE; version 23Q2).[20]

136 2.5 Immunohistochemistry

137 The immunohistochemistry process was conducted in line with previously described

138 methods.[21] Sections were treated with anti-CA9 antibody (#ab184006; Abcam) and

139 subsequently with horseradish peroxidase-conjugated secondary antibody (Nichirei,

140 Tokyo, Japan).

141 2.6 Immunoblot

142 Cells underwent lysis using the RIPA Buffer (FUJIFILM Wako Pure Chemical) infused

143 with a protease inhibitor cocktail (Nacalai Tesque) and a phosphatase inhibitor cocktail

144 (Nacalai Tesque). Equal protein quantities were subjected to SDS-PAGE and transferred

145 onto polyvinylidene fluoride membranes. Post-blocking, the blots were exposed to the

146 designated primary antibody: anti-serpin B9 antibody (#NBP2-93879; Novus

147 Biologicals) or anti-CA9 (#ab184006; Abcam). This was followed by incubation with

148 peroxidase-conjugated goat anti-rabbit IgG secondary antibody (#7074; Cell Signaling

149 Technology). For detection of β-actin, a peroxidase-conjugated anti-β-actin antibody

150 (#017-24573; FUJIFILM Wako Pure Chemical) was used. Protein bands were visualized

151 with the Amersham™ ImageQuant™ 800 (Global Life Sciences Technologies Japan).

6

152   **2.7 Cytotoxicity assays**

153   Young BALB/c mice were immunized with inactivated CT26 cancer cells, as previously

154   described.[22] After a 2-week period, spleen cells were collected and cultured with an H-

155   2L^d-binding peptide (SPSYVYHQF), a tumor antigen AH1 peptide of CT26 derived from

156   the envelope protein (gp70) of an endogenous murine leukemia virus, in the presence of

157   IL-2 (20 U/mL) for 4 days. The AH1 peptide with a purity > 90% was purchased from

158   Invitrogen (Carlsbad). Subsequently, cytotoxicity was assessed using a 5-h ^{51}Cr-release

159   assay, as reported.[22]

160   **2.8 Treatment protocols**

161   To investigate the combined influence of a serpinB9 inhibitor (1,3-benzoxazole-6-

162   carboxylic acid)[23] and anti-PD-1/anti-CTLA-4 antibodies, aged BALB/c mice were

163   inoculated subcutaneously (s.c.) into the flank with RENCA (1×10^6) or RENCA/hCA9

164   (3×10^6) cells. Intraperitoneal (i.p.) injections of the serpinB9 inhibitor (450 μg/mouse),

165   administered twice daily, started on day 3 and continued. On days 10, 13, and 16, mice

166   were given an i.p. injection of both anti-PD-1 mAb and anti-CTLA-4 mAb (150

167   μg/mouse). Equal volumes of rat IgG and hamster IgG were administered as controls.

168   Tumor volume was determined by the formula: volume (mm^3) = (length × width^2) ÷ 2.

169   **2.9 Knockdown of *serpinB9* and mouse *CA9* genes by siRNA transfection**

170   To achieve knockdown of *serpinB9* or mouse *CA9* gene, cancer cells underwent

171   transfection with serpinB9 siRNA or mouse CA9 siRNA using the Lipofectamine

172   RNAiMAX Reagent (Invitrogen). Three distinct SerpinB9 siRNAs and three distinct

173   mouse CA9 siRNAs, along with a control siRNA, were purchased from ORIGENE. After

174   a 2-day interval, cells were harvested.

175   **2.10 Transfection of human and mouse *CA9* genes**

176   The vectors pCMV3-untagged-NCV, pCMV3-hCA9, and pCMV3-mCA9 were

7

177 purchased from Sino Biological Inc. Transfection was conducted with Lipofectamine

178 3000 (Invitrogen). The recombinant DNA experiments were approved by the Shimane

179 University Faculty of Medicine (approval no. 659-1).

2.11 Quantitative RT-PCR

181 Total RNA was extracted with the Nucleozol reagent (Takara), and complementary DNA

182 was synthesized using the ReverTra Ace qPCR RT Master Mix with gNDA Remover

183 (Toyobo), in accordance with the manufacturers' instructions. Quantitative RT-PCR was

184 performed with Thunderbird qPCR Mix (Toyobo). The relative expression levels of target

185 genes were normalized to the level of β-actin using the comparative $2[-\Delta\Delta CT]$ method.

186 The primer sets are listed in Supplemental Table 1.

2.12 *In vitro* culture under hypoxic or acidic conditions

188 For hypoxic culture conditions, cells suspended in RPMI-1640 medium were housed

189 under 1% O_2/94% N_2/5% CO_2 conditions within a humidified automatic O_2/CO_2

190 incubator (Wakenyaku, Japan). To formulate acidic medium, the pH of sodium

191 bicarbonate-free RPMI-1640 medium was adjusted using 1N HCl to values of 6.5, 7.0,

192 and 7.4.

2.13 Survival analysis on clinical data

194 Survival and gene expression data for patients with kidney renal clear cell carcinoma or

195 papillary cell carcinoma were sourced from the Kaplan–Meier plotter database.[24] Based

196 on expression values or ratios, patients were categorized into low or high groups using

197 the best cutoff method.[25]

2.14 Statistical analysis

199 The unpaired two-tailed Student's *t*-test and the Mann–Whitney *U*-test were employed

200 for data analyses between two groups, while the analysis of variance (ANOVA)

201 complemented with the Tukey–Kramer test was used for more than two groups. To

8

1
2
3
4
5
6
7
8
9
10
11
12
13
14
15
16
17
18
19
20
21
22
23
24
25
26
27
28
29
30
31
32
33
34
35
36
37
38
39
40
41
42
43
44
45
46
47
48
49
50
51
52
53
54
55
56
57
58
59
60

202   determine the degree of association between the expression of two genes, Spearman's

203   rank correlation coefficient ρ and the two-tailed P-value were calculated using GraphPad

204   Prism 10.0.1 (GraphPad Software, San Diego, CA, USA). The association between

205   prognostic survival and gene expression was explored by contrasting survival across

206   groups via the Kaplan–Meier plotter analysis. *P* < 0.05 was deemed to indicate statistical

207   significance.

208

209   **3.   RESULTS**

210

211   **3.1 Fewer infiltrating immune cells in RENCA/hCA9 tissues**

212   Although the amino acid sequence of hCA9 shows a 30% divergence from that of mouse

213   CA9, immunohistochemistry indicated a reduced presence of tumor-infiltrating immune

214   cells in RENCA/hCA9 tissues compared to the parental RENCA tissues in aged

215   syngeneic mice.[13] Pursuing this, we evaluated the infiltrating immune cells in both

216   RENCA and RENCA/hCA9 tissues via flow cytometry. The proportions of $CD45^+$

217   immune cells, $CD4^+$ T cells, and $CD11b^+$ $F4/80^+$ cells in RENCA/hCA9 tissues were

218   significantly lower compared to those in RENCA tissues (Figure 1A). The proportions of

219    $CD8^+$ T cells were reduced, but were not significant. Within the $CD45^+$ cells, the

220   percentages of $CD4^+$ T cells were reduced, whereas the percentages of $CD8^+$ T cells and

221    $CD11b^+/F4/80^+$ macrophages showed no notable differences between these tumors

222   (Figure 1B). Figure 1C shows the gating strategy and representative results.

223   **3.2 Increased expression of the *serpinB9* gene in RENCA/hCA9 cells**

224   To investigate the mechanism underlying the reduced immune cell infiltration in

225   RENCA/hCA9 tumors, we first examined whether RENCA/hCA9 cells produce

226   immunosuppressive   factors,   lost   MHC   class   I   expression,   or   expressed

9

227 immunosuppressive molecules. No difference was observed in suppressive activity on T

228 cells or in the expression of MHC class I and PD-L1 between the two cell lines (Figure

229 S1A and B). Subsequently, we compared the gene expression profiles of these cells.

230 Notably, expression of the *serpinB9* gene was significantly elevated in RENCA/hCA9

231 compared to RENCA (Figure 2A). Gene Ontology Enrichment Analysis further

232 highlighted that the most upregulated genes were *serpinB9* genes. These genes encode a

233 molecule that protects cells from natural killer cell-mediated cytotoxicity as a granzyme

234 B inhibitor (Figure 2B). Moreover, data from 43 human RCCs in the CCLE dataset

235 revealed a positive correlation between *CA9* and *serpinB9* gene expression (Figure 2C).

236 However, some cell lines expressed only *CA9* or *serpinB9*.

237

238 **3.3 SerpinB9 contributes to immune resistance to CTL-mediated cytotoxicity**

239 Immunohistochemistry demonstrated that RENCA/hCA9 tissue had higher serpinB9

240 expression compared to RENCA tissue in aged mice (Figure 3A). Since CA9 is a hypoxia-

241 inducible enzyme,[9] we subsequently assessed if hypoxic conditions could stimulate

242 serpinB9 expression in parental RENCA cells. As hypothesized, hypoxic culture

243 enhanced serpinB9 protein expression in both RENCA/hCA9 and parental RENCA cells

244 (Figure 3B). The induction of serpinB9 by hypoxia in RENCA cells was on par with that

245 of DFO, an iron chelator. After confirming that the level of mRNA encoding mouse CA9

246 protein was effectively knocked down via transfection of mouse *CA9* siRNA(C) (Figure

247 3C), RENCA cells were cultured under normoxic or hypoxic conditions; the serpinB9

248 protein expression levels were determined (Figure 3D). Knockdown of the mouse *CA9*

249 gene reduced serpinB9 expression by RENCA cells under hypoxia.

250 Considering the role of serpinB9 in inhibiting lymphocyte-mediated cytotoxicity

251 through the blockage of granzyme B,[16] we then examined if serpinB9 could contribute to

10

252   resistance against CTL-mediated cytotoxicity. Using the AH1 peptide as an antigenic

253   tumor peptide,[22] we compared the sensitivity of AH1 peptide-pulsed RENCA and

254   RENCA/hCA9 cells to AH1 peptide-reactive CTLs sourced from CT26-immunized mice.

255   The data showed RENCA/hCA9 cells were more resilient to these CTLs than RENCA

256   cells (Figure 3E). After validating that serpinB9 siRNA(*C*) effectively knocked down

257   serpinB9 protein expression (Figure 3F), we analyzed the cytotoxicity sensitivity of

258   RENCA/hCA9 cells transfected with either control siRNA or serpinB9 siRNA(*C*). The

259   findings indicated that siRNA-mediated suppression of serpinB9 reinstated the sensitivity

260   of RENCA/hCA9 cells to AH1 peptide-specific CTLs (Figure 3G).

261

262   **3.5 Effect of serpinB9 inhibition on *in vivo* growth of RENCA and RENCA/hCA9 in**

263   **aged mice**

264   We next investigated the therapeutic effects of a serpinB9 inhibitor (1,3-benzoxazole-6-

265   carboxylic acid)[23] on the *in vivo* growth of RENCA and RENCA/hCA9 in aged mice. *In*

266   *vivo* administration of the serpinB9 inhibitor significantly curtailed the growth of RENCA.

267   However, the suppression of RENCA/hCA9 growth was not pronounced (Figure 4A).

268   We also assessed the therapeutic effects of serpinB9 inhibition in combination with anti-

269   PD-1 and anti-CTLA-4 antibodies. The ICB therapy, whether combined with the

270   serpinB9 inhibitor or not, displayed a trend toward inhibiting RENCA/hCA9 growth, but

271   the difference was not statistically significant (Figure 4B).

272

273   **3.6 CA9 induces serpinB9 expression in cancer cells by inducing acidosis**

274   We then sought to determine if induction of either the human or mouse *CA9* gene could

275   stimulate the expression of serpinB9 in parental RENCA cells. After transfecting the

276   human *CA9* gene, we observed an apparent peak in the expression of CA9 protein on day

11

2, which subsequently declined (Figure 5A). Since the anti-CA9 antibody only recognizes the hCA9 protein, no CA9 band was detected in RENCA cells transfected with the mouse *CA9* gene. Interestingly, serpinB9 protein expression began to rise on day 4 following transfection of human or mouse *CA9* genes and persisted until day 6. Quantitative RT-PCR revealed that expression of the *serpinB9* gene was delayed (Figure 5B). To confirm that human *hCA9* gene induction increased serpinB9 expression, we established three new RENCA cell lines expressing that gene (Figure 5C). Although the hCA9 expression levels were relatively low compared with the parental RENCA/hCA9, the new cell lines N1, N2, and N3 exhibited increased serpinB9 protein levels.

CA9 acidifies tumor microenvironments.[14,15] To explore whether this acidification was relevant, RENCA and RENCA/hCA9 cells were cultured in media with or without SB in a CO_2 incubator. In both media, RENCA/hCA9 cell growth was slower than the growth of RENCA cells. However, the pH of SB-free culture supernatants of RENCA/hCA9 cells was lower than the pH of RENCA culture supernatants; this difference was not observed for the SB-containing supernatants (Figure 5D). It has been reported that the pH level in the tumor microenvironment can be below 6.5.[26] Consequently, we cultured RENCA and another mouse carcinoma cell line, CT26, using SB-free medium set at pH levels of 6.5 and 7.5. We discovered that serpinB9 expression was amplified in both cell lines when cultured at pH 6.5 (Figure 5E). This evidence suggests that CA9 elevates the expression of serpinB9 by making the culture conditions more acidic.

3.7 Apoptosis in T cells cultured with RENCA/hCA9

We proceeded to investigate the effects of CA9-induced acidosis on T cell viability *in vitro*. Naïve T cells were prepared and cultured with RENCA or RENCA/hCA9 cells in

12

302   a SB-free medium in a CO_2 incubator. We assessed the apoptosis percentages of T cells

303   and cancer cells when cultured under varying pH conditions in a SB-free medium.

304   Apoptosis of $CD8^+$ T cells was enhanced when cultured at a pH of 6.5 (Figure 5F),

305   indicating the acidic environment impacts T cell apoptosis. Culturing under an acidic

306   condition (pH 6.5) led to apoptosis of cancer cells, albeit at modest levels. Representative

307   results are depicted in Figure S2. Furthermore, RENCA/hCA9 cell culture in SB-free

308   medium for 2 and 4 days was associated with greater levels of apoptosis in both $CD4^+$

309   and $CD8^+$ T cells, compared with RENCA cell culture (Figure 5G). In SB-containing

310   medium, no difference was observed after 2 days of culture, but a significant difference

311   was apparent after 4 days of culture. Representative results can be found in Figure S3.

312   Considering that glycolysis is accelerated in cancer cells and the resulting lactate

313   intensifies acidosis in the tumor microenvironment,[26] we compared lactate levels when

314   RENCA and RENCA/hCA9 cells were cultured in a SB-free medium. However, no

315   significant difference was observed (Figure S4). These findings suggest that hypoxia-

316   induced CA9 amplifies T cell apoptosis in the tumor microenvironment by making the

317   environment more acidic.

318

319   **3.9 Prognosis among RCC patients with elevated *serpinB9* expression**

320   Finally, we explored if variances in *serpinB9* expression influenced the prognosis of RCC

321   patients. Patients were categorized into low and high expression groups based on the

322   optimal cutoff. As previously indicated,[27] clear cell RCC patients with high *CA9*

323   expression had a more favorable overall survival than those with low *CA9* expression

324   (Figure 6A). Conversely, clear cell RCC patients with heightened *serpinB9* expression

325   experienced poorer overall survival than those expressing lower levels of *serpinB9*. When

326   patients were stratified based on high and low serpinB9/CA9 ratios, those with a high

13

327   serpinB9/CA9 ratio faced a worse overall survival than those with a lower serpinB9/CA9

328   ratio (Figure 6B). In contrast, patients with renal papillary cell carcinomas expressing

329   high levels of *CA9* exhibited worse overall survival than patients with low *CA9* expression

330   (Figure 6C). Patients exhibiting higher *serpinB9* expression levels tended to experience

331   worse overall survival than others, but the difference was not statistically significant.

332

4. DISCUSSION

334

335   Although ICB therapy is widely recognized as an effective treatment for various

336   cancers,[1,2] the presence of immune cells at tumor sites is fundamental for its therapeutic

337   efficacy. This underscores the importance of understanding the mechanisms underlying

338   'cold' tumors. In our study, given the reduced infiltration of immune cells in

339   RENCA/hCA9 tissues,[13] we employed this experimental model. Gene microarray

340   analysis identified that the *serpinB9* gene was expressed at significantly higher levels in

341   RENCA/hCA9 cells than in parental RENCA cells. SerpinB9 is an inhibitor of granzyme

342   B, which in turn hampers killer cell-mediated cytotoxicity.[16] Consistent with this, we

343   noted that RENCA/hCA9 cells exhibited a greater resistance to NK cell-mediated

344   cytotoxicity than RENCA cells.[13] In this study, we assessed the resistance of RENCA and

345   RENCA/hCA9 cells to antigen-specific CTLs. Even though RENCA cells express gp70

346   mRNA,[28] we pulsed both RENCA and RENCA/hCA9 cells with the tumor peptide AH1

347   to standardize expression levels of the antigenic peptide. Consequently, RENCA/hCA9

348   cells demonstrated a heightened resistance to AH1 peptide-specific CTLs compared to

349   RENCA cells (Figure 3E). Crucially, the siRNA-mediated suppression of serpinB9 in

350   RENCA/hCA9 cells reinstated their sensitivity to AH1 peptide-specific CTLs (Figure

351   3G).

14

1
2
3
4
5
6
7
8
9
10
11
12
13
14
15
16
17
18
19
20
21
22
23
24
25
26
27
28
29
30
31
32
33
34
35
36
37
38
39
40
41
42
43
44
45
46
47
48
49
50
51
52
53
54
55
56
57
58
59
60

352   A notable observation from our study is the link between hypoxia-inducible CA9

353   expression and an upregulation in serpinB9. In line with this, existing literature indicates

354   that cancer cells grown under hypoxic conditions become more resistant to T cell-

355   mediated destruction.[8,29] Interestingly, hypoxic conditions have been found to either

356   suppress or augment specific T cell functions.[8] However, to our knowledge, this study is

357   the inaugural report proposing that hypoxia-related CA9-induced serpinB9 is, to some

358   extent, associated with immune resistance to CTLs. Yet, the elevated expression of

359   serpinB9 by itself might not sufficiently elucidate why RENCA/hCA9 tumors are 'cold.'

360   This prompted us to explore other potential mechanisms. Observing a delay in the

361   induction of serpinB9 protein and mRNA when RENCA cells were transfected with

362   human or mouse *CA9* genes (Figure 5A and B) led us to hypothesize that CA9 might

363   indirectly stimulate serpinB9 expression. To exclude the possibility that these

364   observations in RENCA/hCA9 cells were off-target effects, we established three new

365   RENCA cell lines stably expressing human CA9; the levels of serpinB9 protein

366   expression increased in all three lines (Figure 5C). This could be through modulation of

367   pH levels of the microenvironment, as CA9 can function as a pH-stat and externally

368   induce acidosis.[14,15] Consequently, considering the role of SB as a pH buffer in a CO_2

369   incubator, we cultured cancer cells in SB-free media. As a result, the pH levels of the

370   culture medium of RENCA/hCA9 cells without SB were lower than that of RENCA cells

371   (Figure 5D, right), and that the *in vitro* culture under acidic condition (pH 6.5) increased

372   the protein expression of mouse serpinB9 (Figure 5E). These lines of evidence support

373   our idea that hypoxia-related CA9 induced serpinB9 expression in cancer cells, at least

374   partially, through acidosis. However, the pH levels of the culture medium of

375   RENCA/hCA9 cells without SB were around 7.23 (Figure 5D, right), and this level was

376   considerably higher than the pH 6.5. Although the pH levels in the vicinity of cell surface

15

might be around pH 6.5, we have no data to explain the discrepancy. On the other hand,

given that the pH levels at the core of tumor tissues are below 6.5,[26] such acidic

microenvironment induced by hypoxia-induced CA9 and glycolysis-mediated lactate

could increase the serpinB9 expression of cancer cells *in vivo*. Further studies are needed.

On the other hand, glycolysis in cancer cells is enhanced, resulting in the production

of lactate, which in turn leads to acidosis.[26] While lactate produced by RENCA cells can

induce acidosis, CA9-expressing RENCA cells further intensify this acidosis through

CA9 activity. Given that the pH levels at the core of tumor tissues are below 6.5,[26] the

acidosis-induced upregulation of serpinB9 could also be prevalent in other types of solid

tumors. Notably, acidic conditions triggered apoptosis in both T cells and cancer cells,

but a pH level of 6.5 amplified apoptosis in CD8^{+} T cells. Even more significant is the

observation that the proportion of apoptotic T cells was higher when co-cultured with

RENCA/hCA9 cells as opposed to co-culture with RENCA cells in a SB-free culture for

2 days (Figure 5G). This heightened apoptosis of T cells may be attributed to the

compounded effects of acidosis, resulting from both hypoxia-induced CA9 and

glycolysis-driven lactate. These insights into acidosis-triggered apoptosis in T cells may

offer valuable clues about the mechanisms underlying 'cold' tumors.

Acidic conditions can augment the expression of serpinB9 in both cancer and

immune cells.[30] Hjelmeland *et al.* reported that acidosis boosts serpinB9 in glioma stem

cells.[31] Furthermore, Jiang *et al.* found that *in vivo* administration of a granzyme B

inhibitor enhances anti-tumor T cell immunity while diminishing immunosuppressive

cells.[23] In our research, we assessed the therapeutic impacts of the same serpinB9 inhibitor

and discovered that its *in vivo* administration considerably hindered the growth of

RENCA. However, it did not notably suppress the growth of RENCA/hCA9, even when

paired with ICB antibodies (Figure 4). Still, this suggests that *in vivo* inhibition of

16

1
2
3
4
5
6
7
8
9
10
11
12
13
14
15
16
17
18
19
20
21
22
23
24
25
26
27
28
29
30
31
32
33
34
35
36
37
38
39
40
41
42
43
44
45
46
47
48
49
50
51
52
53
54
55
56
57
58
59
60

402   serpinB9 does not detrimentally impact anti-tumor immunity. Further exploration is

403   required to fully grasp the implications of serpinB9 inhibition.

404   The proportions of CD4$^+$ T cells were significantly decreased in RENCA/hCA9

405   tissues (Figure 1A and B), but culture under acidic conditions had no effect on apoptosis

406   (Figure 5F). Thus, compared with CD8$^+$ T cells, CD4$^+$ T cells seem to be more susceptible

407   to death in RENCA/hCA9 tissue microenvironments; this difference is not present during

408   *in vitro* culture. In contrast, CD8$^+$ T cells cultured *in vitro* were more acid-sensitive. We

409   have no clear explanation. Further exploratory work is necessary.

410   We examined if the expression levels of *CA9* and *serpinB9* genes affected the

411   prognosis of patients with renal clear cell carcinoma (Figure 6). CA9^{high} cancer patients

412   with renal clear cell carcinoma showed a more favorable prognosis than CA9^{low} patients,

413   aligning with a prior report.[27] Conversely, serpinB9^{high} cancer patients had a less

414   favorable prognosis than serpinB9^{low} patients, a trend also reflected in other studies.[32,33]

415   The serpinB9/CA9 ratio showcased an even more pronounced pattern; a higher ratio

416   indicated a poorer prognosis. Thus, the serpinB9/CA9 ratio in tumor tissues could serve

417   as a biomarker for predicting outcomes in renal clear cell carcinoma patients. On the other

418   hand,   data   from   the   public   Human   Protein   Atlas

419   (https://www.proteinatlas.org/ENSG00000107159-CA9/pathology/renal+cancer)

420   indicate that CA9^{high} renal cancer patients have a worse prognosis than other renal cancer

421   patients. However, these data were derived using all renal cell cancers; we solely focused

422   on renal clear cell carcinomas. Indeed, CA9^{high} renal papillary cell carcinoma patients

423   exhibited worse survival, compared with CA9^{low} patients (Figure 6C). In contrast, CA9^{high}

424   renal clear cell carcinoma patients exhibit a better prognosis than other renal cancer

425   patients.

426   Human serpinB9 is also termed serine proteinase inhibitor 9 (PI-9) and reportedly

17

427   inhibits granzyme B-mediated apoptosis.[34] PI-9 is recognized by the CTLs of epithelial

428   cancer patients; mRNAs encoding PI-9 are expressed in most esophageal, colon, and

429   stomach cancer cell lines.[35] Because hypoxia is a common feature of solid tumors[5,6] and

430   CA9 is a hypoxia-associated protein,[10] CA9-induced induction of serpinB9/PI-9 is not

431   limited to renal cancers.

432   In conclusion, we have identified that hypoxia-associated CA9, through

433   acidification, elevates serpinB9 expression. This makes cancer cells more resilient against

434   antigen-specific CTLs and escalates apoptosis of T cells through acidification. The

435   acidosis induced by CA9 may act in tandem with the lactate produced from glycolysis in

436   cancer cells, amplifying the apoptosis of T cells in the tumor's acidic microenvironment.

437   In this regard, *in vivo* neutralization of acidosis using SB has been shown to bolster anti-

438   tumor responses to ICB therapy in mouse models.[36] We hope our findings shed light on

439   the mechanisms of 'cold' tumors and offer avenues for therapeutic intervention. However,

440   our work had several limitations. We did not examine fresh samples of human renal

441   cancers; the levels of CA9 and PI-9 expression in such samples, and the extent of T cell

442   infiltration, would be informative. Further studies are needed to investigate these aspects.

443

444

445

446

447

448

449

450

451

18

452

Disclosure

454

Conflict of Interest: Mamoru Harada and Yoshihiro Komohara is editorial board members of Cancer Science.

*Ethics Statement

- Approval of the research by an Institutional Review Board, N/A

- Informed Consent, N/A

- Registry and the Registration No. of the study/trial, N/A

- Animal Studies: The experimental protocols were approved by the Committee on the Ethics of Animal Experiments of the Shimane University Faculty of Medicine (IZ3–128, IZ5-52).

*Author Contribution

MH, KY, and HU designed the experiment. MH, HK, YI, and TM carried out the experiments and generated data. RT analyzed the public data. MH drafted the manuscript.

Data availability statement

The RNA array data that support the findings of this study are openly available in figshare at https://figshare.com/s/a929945d1b112b1a44d5

474

475

476

477

19

478

479 **REFERENCES**

480

481   1.   Pardoll DM.The blockade of immune checkpoints in cancer immunotherapy. Nat

482   Rev Cancer. 2012;12(4):252-264.

483   2.   Topalian S, Taube JM, Anders RA, Pardoll DM. Mechanism-driven biomarkers

484   to guide immune checkpoint blockade in cancer therapy. Nat Rev Cancer.

485   2016;16(5):275-287.

486   3.   Bonaventura P, Shekarian T, Alcazer V, et al. Cold Tumors: A Therapeutic

487   Challenge for Immunotherapy. Front Immunol. 2019;10:168.

488   4.   Galon J, Bruni D. Approaches to treat immune hot, altered and cold tumours with

489   combination immunotherapies. Nat Rev Drug Discov. 2019;18(3):197-218.

490   5.   Paredes F, Williams HC, San Martin A: Metabolic adaptation in hypoxia and

491   cancer. Cancer Lett. 2021;502:133-142.

492   6.   Ibrahim-Hashim A, Estrella V. Acidosis and cancer: from mechanism to

493   neutralization. Cancer Metastasis Rev. 2019;38(1-2):149-155.

494   7.   Thews O, Riemann A. Tumor pH and metastasis: a malignant process beyond

495   hypoxia. Cancer Metastasis Rev. 2019;38(1-2):113-129.

496   8.   Vuillefroy de Silly R, Dietrich PY, Walker PR. Hypoxia and antitumor CD8$^+$ T

497   cells: An incompatible alliance? Oncoimmunol. 2016;5(12):e1232236.

498   9.   Rademakers SE, Lok J, van der Kogel AJ, Bussink J, Kaanders JH. Metabolic

499   markers in relation to hypoxia; staining patterns and colocalization of

500   pimonidazole, HIF-1α, CAIX, LDH-5, GLUT-1, MCT1 and MCT4.

501   BMC Cancer. 2011;11:167.

502   10.   Pantuck AJ, Zeng G, Belldegrun AS, et al. Pathobiology, prognosis, and targeted

503   therapy for renal cell carcinoma: exploiting the hypoxia-induced pathway. Clin

504   Cancer Res. 2003;9(13):4641-4652.

505   11.   Pawel Swietach 1, Richard D Vaughan-Jones, Adrian L Harris. Regulation of

506   tumor pH and the role of carbonic anhydrase 9. Cancer Metastasis Rev.

507   2007;26(2):299-310.

508   12.   Uemura H, Fujimoto K, Tanaka M, et al. A phase I trial of vaccination of CA9-

509   derived peptides for HLA-A24-positive patients with cytokine-refractory

510   metastatic renal cell carcinoma. Clin Cancer Res. 2006;12(6):1768-1775.

20

511   13.   Harada M, Iida Y, Kotani H, et al. T-cell responses and combined immunotherapy
512   against human carbonic anhydrase 9-expressing mouse renal cell carcinoma.
513   Cancer Immunol Immunother. 2022;71(2);339-352.

514   14.   Lee SH, McIntyre D, Honess D, et al. Carbonic anhydrase IX is a pH-stat that sets
515   an acidic tumour extracellular pH in vivo. Br J Cancer. 2018;119(5):622-630.

516   15.   Holger M Becker. Carbonic anhydrase IX and acid transport in cancer. Br J Cancer.
517   2020;122(2):157-167.

518   16.   Shresta S, Heusel JW, Macivor DM, Wesselschmidt RL, Russell JH, Ley TJ.
519   Granzyme B plays a critical role in cytotoxic lymphocyte-induced apoptosis.
520   Immunol Rev. 1995;146:211-221.

521   17.   Shimizu K, Uemura H, Yoshikawa M, et al. Induction of antigen specific cellular
522   immunity by vaccination with peptides from MN/CA IX in renal cell carcinoma.
523   Oncol Rep. 2003;10(5):1307-1311.

524   18.   Karasuyama H, Kudo A, Melchers F. The proteins encoded by the V_{preB} and λ_5
525   Pre-B cell-specific genes can associate with each other and with μ heavy chain. J
526   Exp Med. 1990;172:969-972.

527   19.   Zhou Y, Zhou B, Pache L, et al. Metascape provides a biologist-oriented resource
528   for the analysis of systems-level datasets. Nat Commun. 2019;10(1):1523.

529   20.   Ghandi M, Huang FW, Jané-Valbuena J, et al. Next-generation characterization of
530   the Cancer Cell Line Encyclopedia. Nature. 2019;569:503–508.

531   21.   Nakagawa T, Ohnishi K, Kosaki Y, et al. Optimum immunohistochemical
532   procedures for analysis of macrophages in human and mouse formalin fixed
533   paraffin-embedded tissue samples. J Clin Exp Hematop. 2017;57(1):31-36.

534   22.   Ishikawa S, Matsui Y, Wachi S, Yamaguchi H, Harashima N, Harada M. Age-
535   associated impairment of antitumor immunity in carcinoma-bearing mice and
536   restoration by oral administration of *Lentinula edodes* mycelia extract. Cancer
537   Immunol Immunother. 2016;65(8);961-972.

538   23.   Jiang L, Wang YJ, Zhao J. Direct Tumor Killing and Immunotherapy through
539   Anti-SerpinB9 Therapy. Cell. 2020;183(5):1219-1233.e18.

540   24.   Nagy Á, Munkácsy G, Győrffy B. Pancancer Survival Analysis of Cancer
541   Hallmark Genes. Sci Rep. 2021;11(1):6047.

542   25.   Lánczky A, Győrffy B. Web-Based Survival Analysis Tool Tailored for Medical
543   Research (KMplot): Development and Implementation J Med Internet Res.

21

544   2021;23(7):e27633

545   26.   de la Cruz-López KG, Castro-Muñoz LJ, Reyes-Hernández DO, García-Carrancá

546   A, Manzo-Merino J. Lactate in the Regulation of Tumor Microenvironment and

547   Therapeutic Approaches. Front Oncol. 2019;9:1143.

548   27.   Alexander B Stillebroer 1, Peter F A Mulders, Otto C Boerman, Wim J G Oyen,

549   Egbert Oosterwijk. Carbonic anhydrase IX in renal cell carcinoma: implications

550   for prognosis, diagnosis, and therapy. Eur Urol. 2010;58(1):75-83.

551   28.   Iida Y, Harashima N, Motoshima T, et al. Contrasting effects of cyclophosphamide

552   on anti-CTLA-4 blockade therapy in two tumor mouse models. Cancer Sci.

553   2017;108(10):1974–1984.

554   29.   Barsoum IB, Smallwood CA, Siemens DR, Graham CH. A mechanism of hypoxia-

555   mediated escape from adaptive immunity in cancer cells. Cancer Res.

556   2014;74(3):665-674.

557   30.   Mangan MS, Vega-Ramos J, Joeckel LT, et al. Serpinb9 is a marker of antigen

558   cross-presenting dendritic cells. Mol Immunol. 2017;82:50-56.

559   31.   Hjelmeland AB, Wu Q, Heddleston JM, et al. Cell Death Differ. 2011;18(5):829-

560   840.

561   32.   van Houdt IS, Oudejans JJ, van den Eertwegh AJ, et al. Expression of the apoptosis

562   inhibitor protease inhibitor 9 predicts clinical outcome in vaccinated   patients

563   with stage III and IV melanoma. Clin Cancer Res. 2005;11(17):6400-6407.

564   33.   Ibáñez-Molero S, van Vliet A, Pozniak J, et al. SERPINB9 is commonly amplified

565   and high expression in cancer cells correlates with poor immune checkpoint

566   blockade response. Oncoimmunol. 2022;11(1):2139074.

567   34.   Bird CH, Sutton VR, Sun J, et al. Selective regulation of apoptosis: the cytotoxic

568   lymphocyte serpin proteinase inhibitor 9 protects against granzyme B-mediated

569   apoptosis without perturbing the Fas cell death pathway. Mol Cell Biol,

570   1998;18(11):6387-6398.

571   35.   Tanaka K, Harashima N, Niiya F, et al. Serin proteinase inhibitor 9 can be

572   recognized by cytotoxic T lymphocytes of epithelial cancer patients. Jpn J Cancer

573   Res. 2002;93:198-208.

574   36.   Pilon-Thomas S, Kodumudi KN, El-Kenawi AE, et al. Neutralization of Tumor

575   Acidity Improves Antitumor Responses to Immunotherapy. Cancer Res. 2016;

576   76(6):1381-1390.

22

577

FIGURE LEGENDS

579

Figure 1. Fewer infiltrating immune cells in RENCA/hCA9 tissues. (A) Aged mice were s.c. inoculated with RENCA (1×10^6) or RENCA/hCA9 (3×10^6) cells. On day 20, tumor tissues were harvested and analyzed by flow cytometry. (B) Proportions of $CD4^+$ and $CD8^+$ T cells and macrophages among $CD45^+$ cells are shown. Data are presented as mean ± SEM from four mice. *$P < 0.05$, **$P < 0.01$. ns, not significant (Mann–Whitney *U*-test). (B) Gating strategy and representative results are shown.

Figure 2. Increased expression of the *serpinB9* gene in RENCA/hCA9 cells. (A) Gene array analysis was conducted using total RNAs extracted from RENCA and RENCA/hCA9 cells. Red and blue lines indicate four-fold upregulation and downregulation in RENCA/hCA9, respectively. (B) Gene Ontology enrichment analysis of genes with over four-fold upregulated expression was performed using Metascape. (C) The correlation between *CA9* and s*erpinB9* gene expression in 43 human kidney cancer cell lines from the Cancer Cell Line Encyclopedia data (version 23Q2) was assessed, with results shown as a scatter plot. TPM, transcripts per million; ρ, Spearman's rank correlation coefficient.

FIGURE 3. SerpinB9 contributes to immune resistance to CTL-mediated cytotoxicity. (A) Expression of serpinB9 in RENCA and RENCA/hCA9 tissues is displayed. Scale bar, 100 μm. (B) Both RENCA and RENCA/hCA9 cells were cultured under normoxic or hypoxic conditions or treated with deferoxamine (DFO) (100 μg/mL) for 3 days. The harvested cells were tested for protein expression of serpinB9. (C) RENCA cells were transfected with a control or one of three different mouse CA9 siRNAs, then cultured under hypoxic conditions (1% O_2). Quantitative RT-PCR was performed 2 days later. (D) RENCA cells were transfected with control or mouse CA9

23

603   siRNA (*C*) and cultured under normoxic (20% O_2) or hypoxic (1% O_2) conditions. After

604   2 days, the serpinB9 expression levels were determined. (E) The sensitivity of AH1

605   peptide-pulsed RENCA and RENCA/hCA9 cells to AH1 peptide-specific CTLs was

606   determined using a 5 h ^{51}Cr release test. (F) Two days post siRNA transfection,

607   immunoblots were performed to assess expression of serpinB9. Three separate serpinB9

608   siRNAs were transfected. Cont, control. (G) Two days after transfection with serpinB9(C)

609   siRNA, RENCA/hCA9 cells were pulsed with the AH1 peptide and used as targets for

610   AH1 peptide-specific CTLs. *P < 0.05, **P < 0.01 (Student *t*-test). 5 h ^{51}Cr release test

611   was conducted. E/T = effector/target ratio.

612   **Figure 4. Effect of a serpinB9 inhibitor on *in vivo* growth of RENCA and**

613   **RENCA/hCA9 in aged mice.** (A) RENCA (1 × 10^6) or RENCA-hCA9 (3 × 10^6) cells

614   were inoculated s.c. into the flanks of aged mice. The i.p. administration of a serpinB9

615   inhibitor (450 μg/mouse twice daily) began on day 3. Each group comprised 5 mice. Data

616   are presented as means ± SEM. (B) On days 10, 13, and 16, some mice received i.p.

617   injections of anti-PD-1/anti-CTLA-4 antibodies (150 μg/mouse). Results are presented as

618   means ± SEM (Mann–Whitney *U*-test). *P < 0.05. ns, not significant. **P < 0.01.

619   **Figure 5. CA9 increases serpinB9 expression and induces T cell apoptosis through**

620   **acidification.** (A) RENCA cells were transfected with human or mouse CA9 genes. On

621   days 2, 4, and 6, cells were harvested to examine the expression of CA9 and serpinB9.

622   (B) Quantitative RT-PCR was used to determine the levels of mRNAs transcribed from

623   *hCA9*, *mCA9*, and *serpinB9*. (C) The hCA9 and serpinB9 protein levels in RENCA,

624   RENCA/hCA9, and the new hCA9-expressing RENCA cell lines (N1, N2, and N3) were

625   determined. (D) RENCA and RENCA/hCA9 cells were cultured in SB-free or SB-

626   containing medium with CO_2 for 5 days. Cell counts and pH levels of the culture medium

627   are displayed. Data from 3 wells are presented. *P < 0.05, **P < 0.01 (Student's *t*-test).

24

628 (E) RENCA and CT26 cells were cultured under two distinct pH conditions (6.5 and 7.4)

629 using sodium bicarbonate-free medium in a CO_2 incubator for 5 days. Subsequently, cells

630 were harvested to check serpinB9 expression. (F) T cells extracted from naïve BALB/c

631 spleen cells, RENCA, and RENCA/hCA9 cells were cultured under three different pH

632 conditions (6.5, 7.0, and 7.4) in a sodium bicarbonate-free medium in a CO_2 incubator for

633 3 days. T cells, after staining with PE-conjugated anti-CD4 mAb and APC-conjugated

634 anti-CD8 mAb, were then stained with annexin V-FITC and examined via flow cytometry.

635 Cancer cells, post-staining with annexin V-FITC and PI, were analyzed by flow

636 cytometry. (G) T cells purified from naïve BALB/c spleen cells, RENCA, and

637 RENCA/hCA9 cells were co-cultured in a SB-free or SB-containing medium in a CO_2

638 incubator for 2 and 4 days. Post-staining with PE-conjugated anti-CD4 mAb and APC-

639 conjugated anti-CD8 mAb, they were further stained with annexin V-FITC and analyzed

640 by flow cytometry. Data are presented as means ± SD from three samples. *$P < 0.05$,

641 **$P < 0.01$ (Student's t-test). SB, sodium bicarbonate.

642 **Figure 6. Prognosis among RCC patients expressing high *serpinB9* expression.** (A)

643 The Kaplan–Meier plotter univariate analysis illustrates the overall survival duration

644 based on *CA9* mRNA and *serpinB9* mRNA expression in kidney renal clear cell

645 carcinoma patients. (B) Kaplan–Meier plotter univariate analysis represents the overall

646 survival time relative to the ratio of *serpinB9* mRNA/*CA9* mRNA expression in kidney

647 renal clear cell carcinoma patients. (C) The Kaplan–Meier univariate plot reveals the

648 overall survival duration according to the levels of *CA9* mRNA and *serpinB9* mRNA

649 expression in patients with renal papillary cell carcinomas.

650

651

652

25

653

SUPPLEMENTARY INFORMATION

655

Figure S1. No difference in the suppressive ability, MHC class I, and PD-L1

expression between RENCA and RENCA/hCA9 cells.

Figure S2. Effects of pH levels on apoptosis of T cells and cancer cells.

Figure S3. Coculturing with RENCA/hCA9 promotes T cell apoptosis.

Figure S4. Lactate levels in the supernatants from RENCA and RENCA/hCA9 cells.

Table S1. Quantitative PCR primer sequences

26

Figure 1
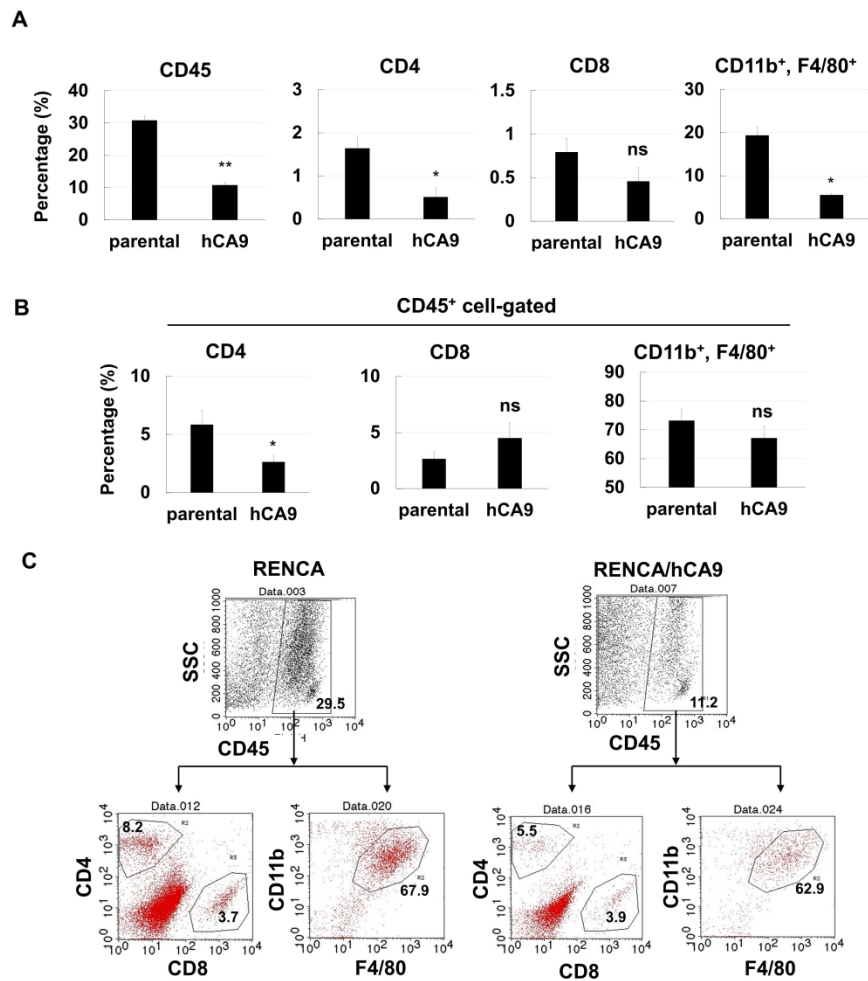
A

B

CD45+ cell-gated

C

Figure 1. Fewer infiltrating immune cells in RENCA/hCA9 tissues. (A) Aged mice were s.c. inoculated with RENCA (1 × 106) or RENCA/hCA9 (3 × 106) cells. On day 20, tumor tissues were harvested and analyzed by flow cytometry. (B) Proportions of CD4+ and CD8+ T cells and macrophages among CD45+ cells are shown. Data are presented as mean ± SEM from four mice. *P < 0.05, **P < 0.01. ns, not significant (Mann–Whitney U-test). (B) Gating strategy and representative results are shown.

950x1249mm (96 x 96 DPI)

1
2
3
4
5
6
7
8
9
10
11
12
13
14
15
16
17
18
19
20
21
22
23
24
25
26
27
28
29
30
31
32
33
34
35
36
37
38
39
40
41
42
43
44
45
46
47
48
49
50
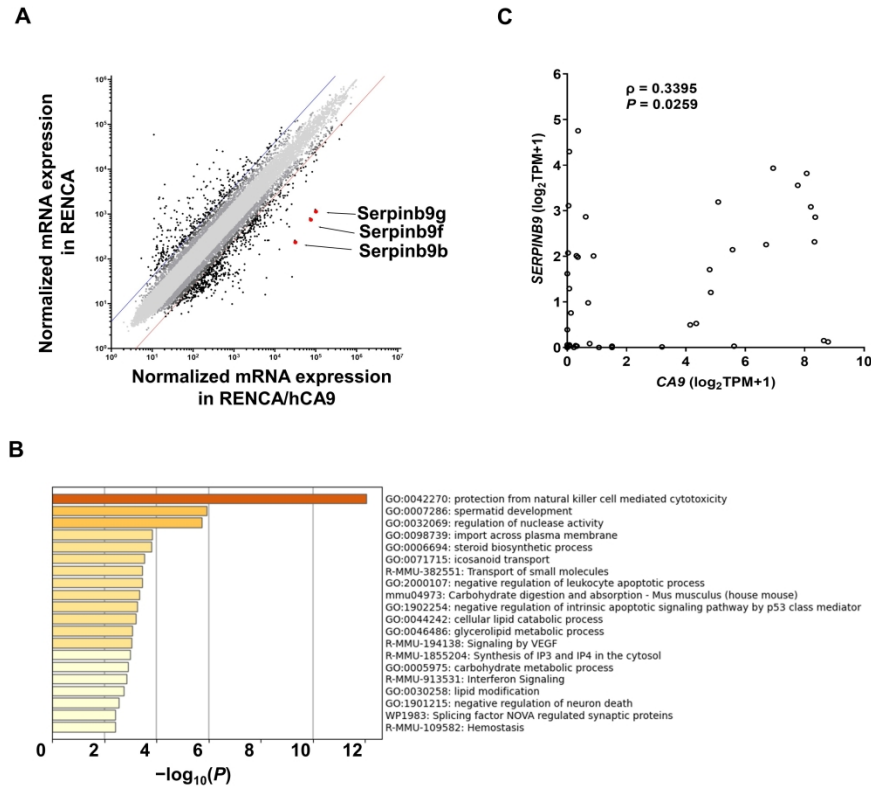51
52
53
54
55
56
57
58
59
60

Figure 2

Figure 2. Increased expression of the serpinB9 gene in RENCA/hCA9 cells. (A) Gene array analysis was conducted using total RNAs extracted from RENCA and RENCA/hCA9 cells. Red and blue lines indicate four-fold upregulation and downregulation in RENCA/hCA9, respectively. (B) Gene Ontology enrichment analysis of genes with over four-fold upregulated expression was performed using Metascape. (C) The correlation between CA9 and serpinB9 gene expression in 43 human kidney cancer cell lines from the Cancer Cell Line Encyclopedia data (version 23Q2) was assessed, with results shown as a scatter plot. TPM, transcripts per million; ρ, Spearman's rank correlation coefficient.

950x1249mm (96 x 96 DPI)

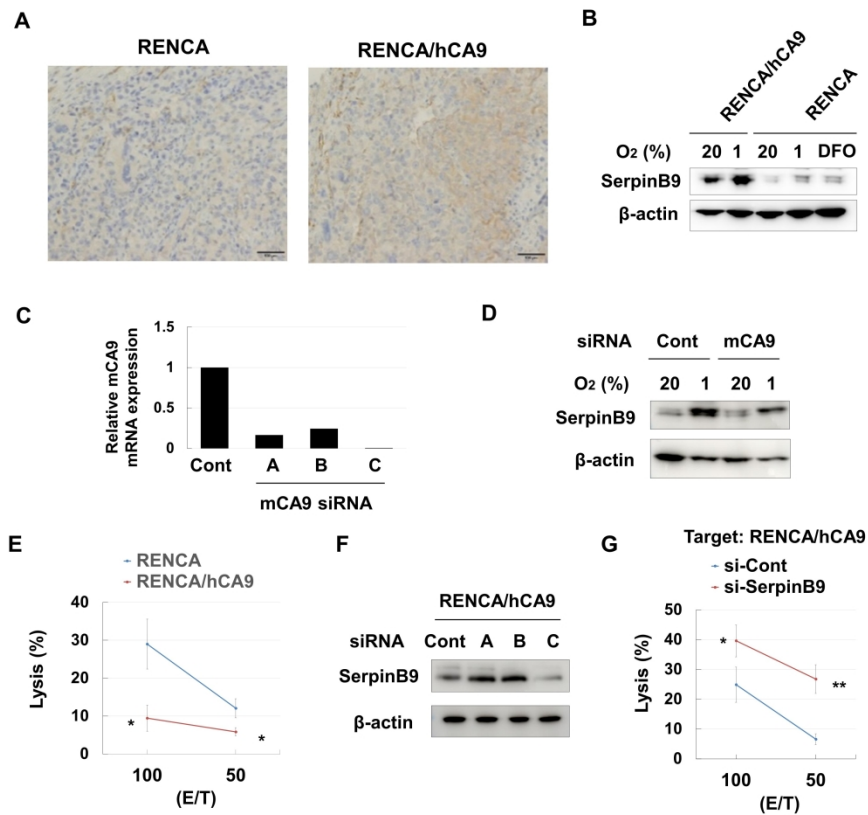Cancer Science

Figure 3

FIGURE 3. SerpinB9 contributes to immune resistance to CTL-mediated cytotoxicity. (A) Expression of serpinB9 in RENCA and RENCA/hCA9 tissues is displayed. Scale bar, 100 □m. (B) Both RENCA and RENCA/hCA9 cells were cultured under normoxic or hypoxic conditions or treated with deferoxamine (DFO) (100 □g/mL) for 3 days. The harvested cells were tested for protein expression of serpinB9. (C) RENCA cells were transfected with a control or one of three different mouse CA9 siRNAs, then cultured under hypoxic conditions (1% O2). Quantitative RT-PCR was performed 2 days later. (D) RENCA cells were transfected with control or mouse CA9 siRNA (C) and cultured under normoxic (20% O2) or hypoxic (1% O2) conditions. After 2 days, the serpinB9 expression levels were determined. (E) The sensitivity of AH1 peptide-pulsed RENCA and RENCA/hCA9 cells to AH1 peptide-specific CTLs was determined using a 5 h 51Cr release test. (F) Two days post siRNA transfection, immunoblots were performed to assess expression of serpinB9. Three separate serpinB9 siRNAs were transfected. Cont, control. (G) Two days after transfection with serpinB9(C) siRNA, RENCA/hCA9 cells were pulsed with the AH1 peptide and used as targets for AH1 peptide-specific CTLs. *P < 0.05, **P < 0.01 (Student t-test). 5 h 51Cr release test was conducted. E/T = effector/target ratio.

1
2
3
4
5
6
7
8
9
10
11
12
13
14
15
16
17
18
19
20
21
22
23
24
25
26
27
28
29
30
31
32
33
34
35
36
37
38
39
40
41
42
43
44
45
46
47
48
49
50
51
52
53
54
55
56
57
58
59
60

950x1249mm (96 x 96 DPI)

1
2
3
4
5
6
7
8
9
10
11
12
13
14
15
16
17
18
19
20
21
22
23
24
25
26
27
28
29
30
31
32
33
34
35
36
37
38
39
40
41
42
43
44
45
46
47
48
49
50
51
52
53
54
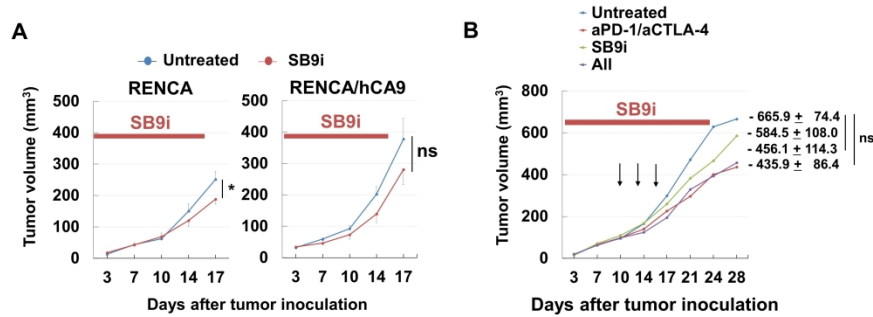55
56
57
58
59
60

Figure 4

Figure 4. Effect of a serpinB9 inhibitor on in vivo growth of RENCA and RENCA/hCA9 in aged mice. (A) RENCA (1 × 106) or RENCA-hCA9 (3 × 106) cells were inoculated s.c. into the flanks of aged mice. The i.p. administration of a serpinB9 inhibitor (450 □g/mouse twice daily) began on day 3. Each group comprised 5 mice. Data are presented as means ± SEM. (B) On days 10, 13, and 16, some mice received i.p. injections of anti-PD-1/anti-CTLA-4 antibodies (150 μg/mouse). Results are presented as means ± SEM (Mann–Whitney U-test). *P < 0.05. ns, not significant. **P < 0.01.
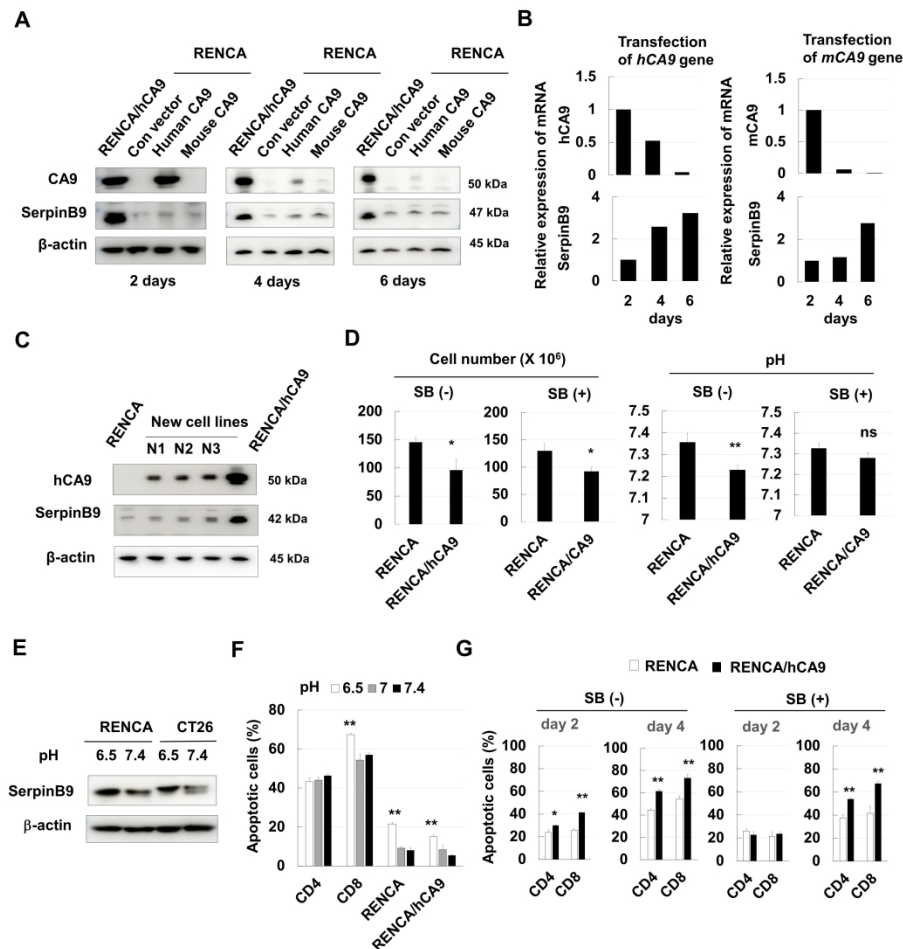
950x1249mm (96 x 96 DPI)

Figure 5

Figure 5. CA9 increases serpinB9 expression and induces T cell apoptosis through acidification. (A) RENCA cells were transfected with human or mouse CA9 genes. On days 2, 4, and 6, cells were harvested to examine the expression of CA9 and serpinB9. (B) Quantitative RT-PCR was used to determine the levels of mRNAs transcribed from hCA9, mCA9, and serpinB9. (C) The hCA9 and serpinB9 protein levels in RENCA, RENCA/hCA9, and the new hCA9-expressing RENCA cell lines (N1, N2, and N3) were determined. (D) RENCA and RENCA/hCA9 cells were cultured in SB-free or SB-containing medium with CO2 for 5 days. Cell counts and pH levels of the culture medium are displayed. Data from 3 wells are presented. *P < 0.05, **P < 0.01 (Student's t-test). (E) RENCA and CT26 cells were cultured under two distinct pH conditions (6.5 and 7.4) using sodium bicarbonate-free medium in a CO2 incubator for 5 days. Subsequently, cells were harvested to check serpinB9 expression. (F) T cells extracted from naïve BALB/c spleen cells, RENCA, and RENCA/hCA9 cells were cultured under three different pH conditions (6.5, 7.0, and 7.4) in a sodium bicarbonate-free medium in a CO2 incubator for 3 days. T cells, after staining with PE-conjugated anti-CD4 mAb and APC-conjugated anti-CD8 mAb, were then stained with annexin V-FITC and examined via flow cytometry. Cancer cells, post-staining with annexin V-FITC and PI, were analyzed by flow cytometry. (G) T cells purified from

1
2
3
4
5
6
7
8
9
10
11
12
13
14
15
16
17
18
19
20
21
22
23
24
25
26
27
28
29
30
31
32
33
34
35
36
37
38
39
40
41
42
43
44
45
46
47
48
49
50
51
52
53
54
55
56
57
58
59
60

naïve BALB/c spleen cells, RENCA, and RENCA/hCA9 cells were co-cultured in a SB-free or SB-containing medium in a CO_2 incubator for 2 and 4 days. Post-staining with PE-conjugated anti-CD4 mAb and APC-conjugated anti-CD8 mAb, they were further stained with annexin V-FITC and analyzed by flow cytometry. Data are presented as means ± SD from three samples. *$P < 0.05$, **$P < 0.01$ (Student's t-test). SB, sodium bicarbonate.

950x1249mm (96 x 96 DPI)
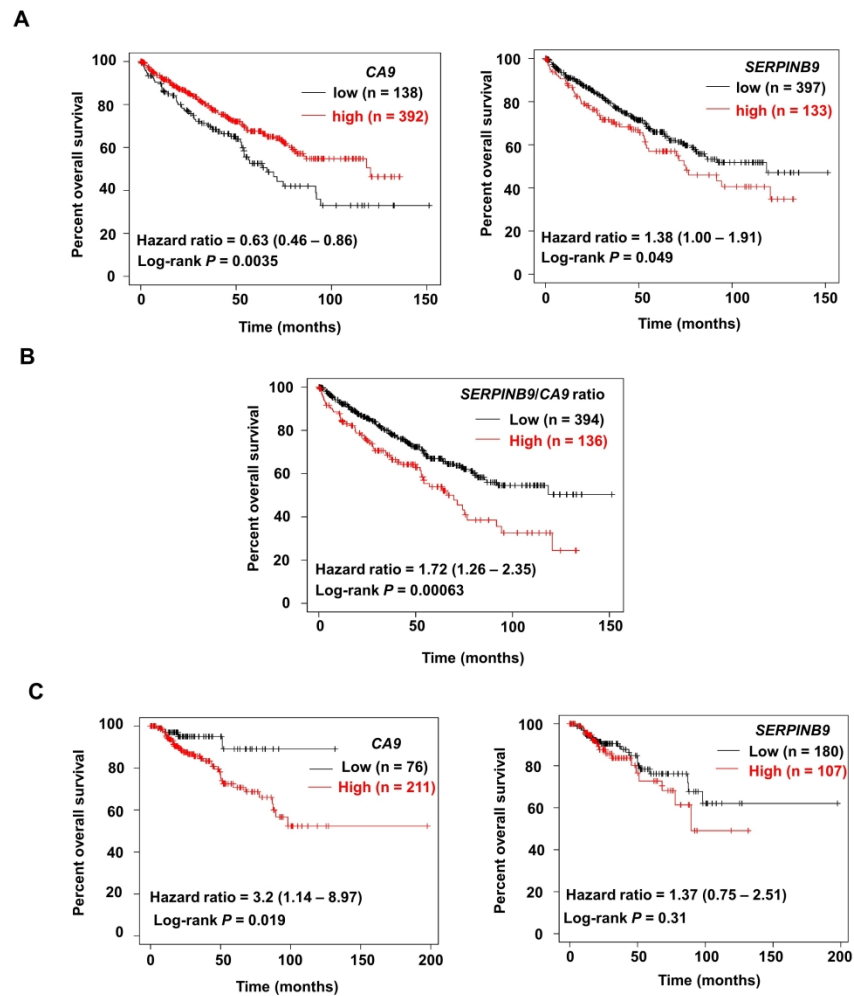
Figure 6

A

B

C

Figure 6. Prognosis among RCC patients expressing high serpinB9 expression. (A) The Kaplan–Meier plotter univariate analysis illustrates the overall survival duration based on CA9 mRNA and serpinB9 mRNA expression in kidney renal clear cell carcinoma patients. (B) Kaplan–Meier plotter univariate analysis represents the overall survival time relative to the ratio of serpinB9 mRNA/CA9 mRNA expression in kidney renal clear cell carcinoma patients. (C) The Kaplan–Meier univariate plot reveals the overall survival duration according to the levels of CA9 mRNA and serpinB9 mRNA expression in patients with renal papillary cell carcinomas.

950x1249mm (96 x 96 DPI)